



HAL
open science

Single Crystal and Sintered Alumina Corrosion in Liquid Sodium

Jean-Louis Courouau, Marlu-Cesar Steil, Jacques Fouletier, Fabien Rouillard,
Véronique Lorentz, Patrick Bonnaille, Anthony Muccioli, Jonathan Unger,
Sandy Tricoit, Michel Tabarant

► **To cite this version:**

Jean-Louis Courouau, Marlu-Cesar Steil, Jacques Fouletier, Fabien Rouillard, Véronique Lorentz, et al.. Single Crystal and Sintered Alumina Corrosion in Liquid Sodium. *Oxidation of Metals*, 2017, 87 (5-6), pp.789-800. 10.1007/s11085-017-9743-3 . cea-02388860v1

HAL Id: cea-02388860

<https://cea.hal.science/cea-02388860v1>

Submitted on 17 Mar 2020 (v1), last revised 17 Jun 2020 (v2)

HAL is a multi-disciplinary open access archive for the deposit and dissemination of scientific research documents, whether they are published or not. The documents may come from teaching and research institutions in France or abroad, or from public or private research centers.

L'archive ouverte pluridisciplinaire **HAL**, est destinée au dépôt et à la diffusion de documents scientifiques de niveau recherche, publiés ou non, émanant des établissements d'enseignement et de recherche français ou étrangers, des laboratoires publics ou privés.

Single crystal and sintered alumina corrosion in liquid sodium

J.-L. Courouau, M.-C. Steil, J. Fouletier, F. Rouillard, V. Lorentz, P. Bonnaillie, A. Muccioli, J. Unger, S. Tricoit, M. Tabarant

► **To cite this version:**

J.-L. Courouau, M.-C. Steil, J. Fouletier, F. Rouillard, V. Lorentz, et al.. Single crystal and sintered alumina corrosion in liquid sodium. Oxidation of Metals, Springer Verlag, 2016. hal-02445715

HAL Id: hal-02445715

<https://hal-cea.archives-ouvertes.fr/hal-02445715>

Submitted on 20 Jan 2020

HAL is a multi-disciplinary open access archive for the deposit and dissemination of scientific research documents, whether they are published or not. The documents may come from teaching and research institutions in France or abroad, or from public or private research centers.

L'archive ouverte pluridisciplinaire **HAL**, est destinée au dépôt et à la diffusion de documents scientifiques de niveau recherche, publiés ou non, émanant des établissements d'enseignement et de recherche français ou étrangers, des laboratoires publics ou privés.

Letter to the conference organization:

The abstract that was accepted and that will be presented in the poster is: ‘Ceramic corrosion in liquid sodium: Alumina, hafnia and zirconia ceramics behaviour at 450°C and 550 °C in static conditions’.

However, we chose to focus the paper on the alumina and homogenous corrosion rates as the results deserved to our opinion to be treated in them self without being too general. We hope that you will agree with this modification.

The authors.

Publication in the journal 'Oxidation of Metals' (Peer-reviewed)

Single crystal and sintered alumina corrosion in liquid sodium

Jean-Louis COUROUAU^a, Marlu-César STEIL^{b,c}, Jacques FOULETIER^{b,c}, Fabien ROUILLARD^a, Véronique LORENTZ^a, Patrick BONNAILLIE^d, Anthony MUCCIOLI^a, Jonathan UNGER^a, Sandy TRICOIT^a, Michel TABARANT^e

^a*Den-Service de la Corrosion et du Comportement des Matériaux dans leur Environnement (SCCME), CEA, Université Paris-Saclay, F-91191, Gif-sur-Yvette, France*

^b*Univ. Grenoble Alpes, LEPMI, F-38000 Grenoble, France*

^c*CNRS, LEPMI, F-38000 Grenoble, France*

^d*Den-Service de Recherches de Métallurgie Physique (SRMP), CEA, Université Paris-Saclay, F-91191, Gif-sur-Yvette, France*

^e*Den-Service d'Etudes Analytiques et de Réactivité des Surfaces (SEARS), CEA, Université Paris-Saclay, F-91191, Gif-sur-Yvette, France*

jean-louis.courouau@cea.fr; cesar.steil@lepmi.grenoble-inp.fr; jacques.fouletier@lepmi.grenoble-inp.fr; fabien.rouillard@cea.fr; veronique.lorentz@cea.fr; patrick.bonnaillie@cea.fr; anthony.muccioli@edf.fr; jonathan.unger@cea.fr; sandy.tricoit1@areva.com; michel.tabarant@cea.fr

Abstract. Corrosion tests were achieved in static conditions at 450 and 550 °C for various oxygen contents and durations with single crystal and sintered alumina regarded as model materials for ceramics. Extremely pure and dense sintered alumina presented no intergranular corrosion and identical behavior as alumina single crystal. Corrosion appeared to proceed by reaction of Al₂O₃ with dissolved oxygen (Na₂O) to form sodium aluminate (NaAlO₂). Then, sodium aluminate dissolved or reduced in liquid sodium upon a mechanism still to elucidate. The corrosion morphology appeared as equivalent to dissolution, whose rates were assessed from weight loss measurement supposing linear kinetics: 0.07 to 1.4 μm/y at 450 and 550 °C and low oxygen content. The apparent activation energy was measured to be approximately 130 kJ/mol. A first order reaction kinetics with respect to oxygen content was found. At 550 °C and low oxygen, the dissolution rate of sintered alumina appeared to be approximately twice higher than the one of single crystal, likely because of the highest corrosion rate of grain boundaries.

Keywords: alumina, sodium, corrosion, kinetics

INTRODUCTION

The use of liquid sodium at high temperature as a coolant in systems such as Sodium Fast Reactor (SFR) [1], concentrated solar power, heat pipes, etc., requires that liquid metal and materials interactions must be well understood in order to be able to predict the corrosion and to guarantee the service life-time of the component. Ceramic oxides are envisaged for monitoring the dissolved oxygen content of the liquid metal (oxygen sensor: ThO₂-, HfO₂- and ZrO₂-based electrolytes), or, alongside alumina for the catching of the molten core material (corium) in case of a nuclear meltdown [2-5]. Both applications require that the ceramics material be compatible with the liquid metal in conditions and durations corresponding to the application: 250 to 400 °C for low duration (1000 h at least) for sensors, and 400 °C for 60 years for the core catcher. For this latter, even though direct contact of the ceramic materials with sodium will probably be prevented by the use of steel cladding or steel deposits, the ceramic oxides ability to withstand the liquid sodium corrosion must be demonstrated from a safety point of view. In both cases, the dissolved oxygen concentrations as well as the sodium velocity are expected to be low (< 10 ppm, ~cm/s) in the normal operating conditions. Over the extended service lifetime of the reactor, some incidental conditions should also be taken into account for the long term corrosion prediction, such as some events at higher than expected oxygen levels (15 ppm

for 100 h [2]). Indeed, the core catcher cannot be repaired nor replaced, so that its service lifetime defines the reactor's lifetime. The lacks of understanding and specific data for these ceramics justify why these materials are not used in SFR built reactors. In previous works we demonstrated that the microstructure of the ceramic was a key factor for corrosion resistance in sodium liquid [4, 5]. The object of the present paper was to study the alumina behavior in liquid sodium. In this context, the single crystal and high purity sintered alumina could be regarded as a model for the studies of homogenous corrosion by the liquid sodium.

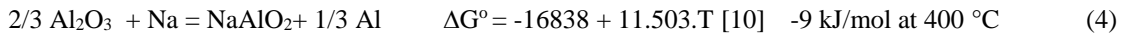
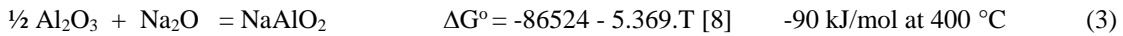
CERAMIC MATERIALS AND LIQUID SODIUM ISSUE

The main corrosion mechanism of ceramic by liquid sodium are as follows: thermomechanical effects such as those related to temperature change inducing a potential sensitivity to thermal shocks, localized corrosion at grain boundaries that involves both intergranular corrosion (IGC) and liquid metal penetration, homogeneous corrosion at interfaces in contact with liquid sodium as well as with trace impurities such as dissolved oxygen, and reduction of the ceramic oxide by liquid sodium. The IGC is particularly damaging since once initiated over a depth of several grains, rows of grains could detach, leading to large weight loss or even to the complete disintegration of the specimen over a relatively short time. According to Kano and Mayer [6, 7], trace impurities in ceramic, such as silica (SiO_2) plays a major role in its occurrence: silica is said to segregate at grain boundaries and to preferentially react with liquid metal or with dissolved oxygen according to the following thermodynamically possible reactions (free enthalpies from [8]):



Kinetics is fast above 300°C [9]. Sodium silicate ($\text{Na}_2\text{O} \cdot \text{SiO}_2$) forms probably a liquid phase at the grain boundary and is highly soluble in liquid sodium. It most probably favors liquid metal penetration and affects grain cohesion. In the tests reported by Kano [6], the alumina with trace levels of impurities below 100 ppm presented negligible intergranular corrosion after 1000 h in liquid sodium at 650°C and 1 ppm of oxygen.

The homogeneous corrosion refers to reaction of the substrate with liquid sodium or its impurities at the interface according to reaction similar to equations (1) and (2) producing the more thermodynamically stable sodium aluminate (NaAlO_2):



The only ternary oxide taken into account here are those of the lowest stoichiometry, supposed as the most stable: $(\text{Na}_2\text{O})_x \cdot (\text{M}_y\text{O}_z)$, x being the lowest value. All other compounds such as sodium silico-aluminate ($\text{Na}_2\text{O} \cdot \text{Al}_2\text{O}_3 \cdot 2\text{SiO}_2$) are neglected for the moment. The available literature data suggest that the kinetics of reaction of these thermodynamically more stable oxides are slow. Jung [9] observed the formation of sodium aluminate scale with a colored alumina zone underneath on high density and high purity alumina specimen immersed in static condition at 900°C in oxygen saturated sodium, conditions that are extremely severe. The aluminate thickness appeared to increase with increasing test duration ($400 \mu\text{m}$ -100 h). For the less severe testing conditions encountered in Kano's study [6], no surface layer nor colored zone could be observed after 1000 h at 650°C and 1 ppm oxygen, and small weight loss was systematically measured. Although oxygen plays a critical role in these corrosion mechanisms, it is not well documented in the literature, as the reactants are not identified. The surface reaction appears as similar to oxidation, followed eventually by a step of oxide reduction or dissolution into the liquid metal. There is a possibility of sodium aluminate hydrolysis in the aqueous solution used to remove sodium residue. The apparent 'dissolution' reaction is then characterized by weight loss, as measured by Kano [6] and should present a receding interface. Jung [9] observed the formation of thick sodium aluminate layer, either because the volume of the test capsule was small so that the liquid metal got quickly saturated in dissolved sodium aluminate oxide, or because the conditions were extremely severe both in temperature and in oxygen content, or for both reasons. Lastly, sodium may reduce the oxide substrate because of its high reducing oxygen potential, leading to the formation of metal (Al) as well as to the formation of point defects, also known as colored centers or 'F'centers ($\text{V}_\text{O}^\bullet$ according to the Kröger & Vink notation). This

blackened surface layer presents a thickness that increases with temperature and exposure time [9], but only a small fraction of the vacancies are involved. Heat treatment of the specimen (800 °C – 2 h) after the sodium test corresponds to the re-oxidation: weight gain appears indeed as negligible [9]. However, if its effect on the mechanical properties is unknown, its effect on the electrical properties is an increase of the electronic conduction. All of these interactions are additionally influenced by the porosity and the microstructure of the ceramic oxide that is little documented in the literature too.

High density and high purity polycrystalline sintered α -alumina as well as single crystals of alumina were chosen for the studies of homogenous corrosion by the liquid sodium in order to first sort out the effect of the liquid metal on alumina substrate independently of microstructure and grain boundaries related effects.

EXPERIMENTAL PROCEDURES

Sintered ceramics with no open porosity and high chemical purity (> 99.7 % in weight) was supplied by UMICORE (DEGUSSIT AL23 grade: 60 $\mu\text{g/g}$ of SiO_2 , 90 $\mu\text{g/g}$ of CaO , 190 $\mu\text{g/g}$ of Fe_2O_3 , 500 $\mu\text{g/g}$ of Na_2O , 1460 $\mu\text{g/g}$ of MgO , 300 $\mu\text{g/g}$ of K_2O [7]) in the shape of tubes of 1.95 mm internal diameter and 3.9 mm external diameter for about 20 mm in length. The mean grain size was 10 μm . Single crystal of alumina was supplied by Rubis SA in the form of rod of 20 mm in diameter, cut with diamond disk with no further preparation other than degreasing.

TABLE 1. Test conditions in static liquid sodium.

Temperature	[O]	Durations (h)
450 °C	< 0.1 ppm	250-500-1000-2000-4000 h
450 °C	~ 40 ppm-	1000 h
550 °C	< 0.1 ppm	3400 h
550 °C	1-5 ppm	650-1500-3050-3950-4600 h
550 °C	~ 40 ppm	2000 h
550 °C	~ 240 ppm	250 h

The tests were run in the test bench called “CORRONa”[2, 11]. The sodium was contained in a molybdenum crucible. A furnace heated the thermal well where the crucible was set. All of this was set below an argon purified glove box that simplifies all operations required for preparation of the test and handling of the liquid metal. During corrosion test, the system was perfectly tight towards both the atmosphere and the argon of the gloves box. Before testing, the 99.95 % pure sodium (Métaux Spéciaux - ER grade) was melted and the free level was skimmed off in order to remove sodium oxide present in excess. A low temperature step at 105 °C was done for 300 h, analog to a decantation step, followed by the skimming off any residual oxides present at the free level. Then, a last purification step was done at high temperature (628 °C during 75 h) with large surface zirconium foil (150 x 300 x 0.125 mm - Neyco) to getter any residual oxygen. This foil was removed after the purification step and sometimes replaced with a new one to maintain as low as possible the oxygen concentration. Oxygen was then assessed to 0.1 ppm or lower while, without the Zr getter during the sodium test, the oxygen was assessed to 1-5 ppm. The qualitative appearance of the free level confirmed this assessment as perfect mirror is obtained. This latter purification step allowed to assess the amount of oxygen present in the liquid metal when no Zr purification was done to roughly 40 ppm, as the first test were done at a moment when the zirconium purification step was not yet implemented as a routine operation. The 200 ppm oxygen condition was obtained by adding after the zirconium purification step the required amount of sodium oxide to the liquid metal (Na_2O - Alfa Aesar). It must be noticed that pure new sodium is carburizing, meaning a high carbon activity [12, 13]. The specimens were then immersed in liquid sodium at 110 °C and the system was tightly closed so that the liquid metal equilibrates with the argon cover gas that prevents any further contamination by the cover gas on the long term. Sodium was heated to 450 °C or 550 °C at 0.5 °C/min, and the temperature was kept constant for the duration required. Temperature was then decreased at 0.5 °C/min to remove one set of samples and possibly replace by a new set. Most of the time, other specimens were exposed during the same tests, mainly steels (316L(N), Fe-9Cr-1Mo, 800 alloys, pure Ni, Fe, etc.) or ceramic materials (zirconia, hafnia). The surface over volume ratio averaged 0.9 dm^{-1} , mainly due to the steels specimens neglecting the Mo crucible surface. After immersion in liquid sodium, the specimens were washed with 99.9 % pure ethanol (Carlo Erba supplier) in order to remove metallic sodium residue from the sample surface and were stored in desiccators. After the first washing and weighting, a second rapid cleaning in pure water was performed. Table 1 recalls the testing conditions achieved.

The specimens were then weighted to get the weight variation. Morphological characterizations were performed by means of electron microscopy: Scanning Electron Microscopy (SEM), the device Zeiss - Gemini ultra 55 was used to characterize surface and specimen cross-sections. In both cases, Energy Dispersive X-ray analyses were done (EDX, device: Bruker AXS Flash Detector 4010). Cross-sections were prepared by fracture in order to assess the fracture mode as an indication of the liquid metal penetration and reaction at grain boundaries.

RESULTS AND DISCUSSION

Table 2 presents a synthesis of the weight variation measured for the various specimens after the first cleaning in ethanol and the second cleaning with pure water. The weight variation equals the difference between the final and initial weights, in order to measure the weight loss. Negative value means a weight gain. Accuracy of the balance was about $\pm 30 \mu\text{g}$. The macroscopic change of alumina materials through sodium exposure appeared as limited, as almost no change in color was observed. All specimen color was grayish after the first ethanol cleaning, but returned to white after a second more efficient pure water cleaning. Single crystal surface that was originally mirror-polished turned to a de-polished surface.

TABLE 2. Alumina weight loss in relation to test conditions in static liquid sodium.
(* : 2 specimens tested for the same exposure time; ' one at the beginning of the test and the latter at the end).

Materials	Specimen geometry	Sodium temperature ($^{\circ}\text{C}$)	Time of exposure (h)	Oxygen content (ppm)	Weight loss after 1 st cleaning (mg/dm^2)	Weight loss after 2 nd cleaning (mg/dm^2)
Sintered alumina	Tube	550	660*'	1-5	4.07 – 7.86	3.7 – 8.25
			1550*'		-12.14 – 3.88	2.86 – 17.09
			3025*'		-45.63 – 34.97	14.04 – 35.76
			3920*'		-195.59 – 28.23	24.59 – 28.84
			4577*'		29.45	30.67 – 29.21
Sintered alumina	Tube	450	1000	40		0.43 – 0.57
Sintered alumina	Tube	450	243*	0.1	-4.69 – -11.71	1.45 – 1.37
		494*	-4.12 – -4.21		1.59 – 1.89	
		994*	-27.88 – -39.06		1.04 – 0.91	
		1994*	1.32 – 1.70		1.61 – 2.67	
		3996*	-6.69 – -10.55		0.84 – 0.33	
Single crystal	disk or ½ disk	550	1549	1-5	-13.08	0.46
			3028		-28.69	22.14
			4577		-12.31	10.46
Single crystal	disk	550	2000	40		38.84
Single crystal	disk	550	3400	0.1		3
Single crystal	disk	550	250	240		28.3

These weight evolution were directly related to the amount of sodium residues and reaction products remaining on the specimen. Scanning electron microscopic (SEM) observations (Figure 1 and Figure 2) of the surface layer, or of cross-section obtained by fracture clearly demonstrated the formation of porosities in the surface layer. After the second cleaning, the weight variation changed its sign, from weight gain to weight loss for sintered alumina and single crystal. The cleaning steps appeared, then, as critical to ensure the correct monitoring of the corrosion. It was assumed that the second water cleaning procedure (pure water – 15 minutes – ultrasonic bath) was efficient enough to get representative weight variation. Additional tests were done with specimens of the $450^{\circ}\text{C} - 0.1 \text{ ppm}$ corrosion test that supported this hypothesis within roughly 10-100% of the weight loss. Indeed, some specimens presented almost no variation upon subsequent 3rd cleaning with water and high temperature stage ($800^{\circ}\text{C} - 3 \text{ h}$) with 10% increase, while some others presented either a large increase or a large decrease (100 %). These difficulties in measuring representative weight variations explained the scattering of the weight loss data, but it was assumed that the number

of specimens gave mean value statistically representative of the actual weight loss. In addition, initial stage of the corrosion can affect the time to attain steady state corrosion (wetting conditions, etc.), which is an additional source of scattering.

The morphology of corrosion for sintered and single crystal alumina appeared as almost identical as seen on Figure 1 for a weight loss within the same order of magnitude. This demonstrated that the pure and dense sintered alumina presents the same behavior as the single crystal to the condition that the grain boundary corrosion is negligible, which is the case for this high purity grade of sintered alumina.

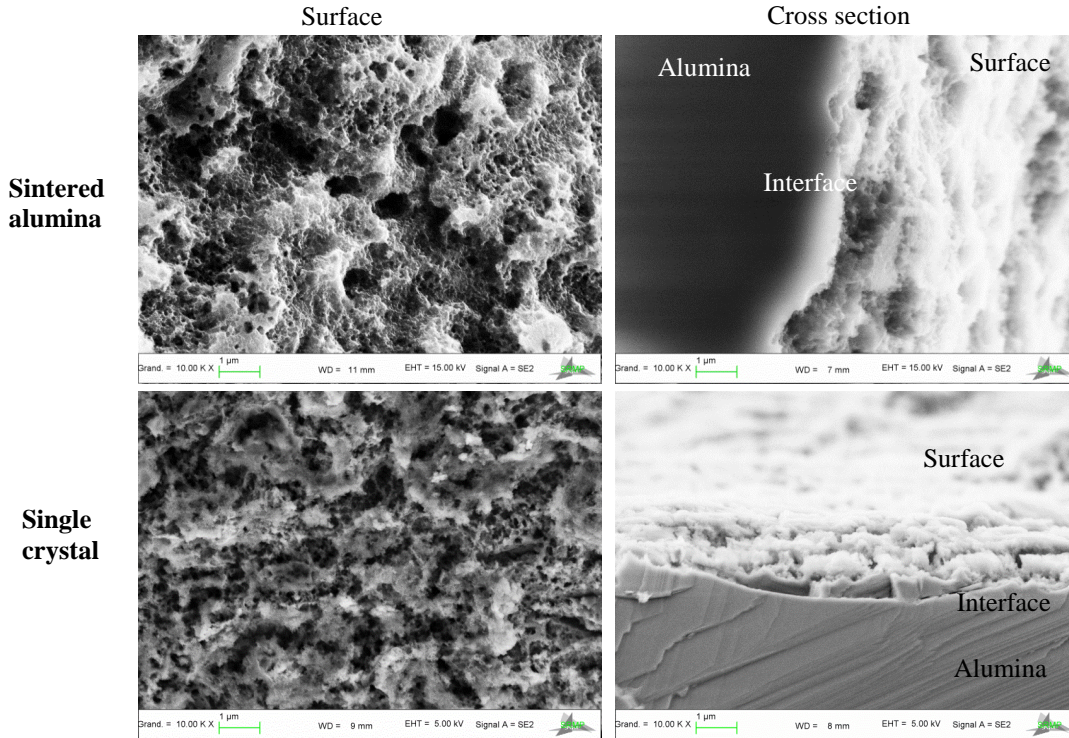


FIGURE 1. SEM observations of surface and fractured cross section of the sintered alumina and single crystal after immersion in liquid sodium at 550 °C, 1-5 ppm of oxygen and 3028 h.

The apparent porosity of the surface layer tended to increase with exposure duration in liquid sodium as well as with temperature. The fracture surface kept being trans-granular for all conditions up to the interface (Figure 2), demonstrating no intergranular corrosion. Porosities appeared as preferentially formed at grain boundaries as observed in Figure 2 on sintered alumina. This effect was expected as grain boundaries are thought to offer lower energy sites for corrosion attack.

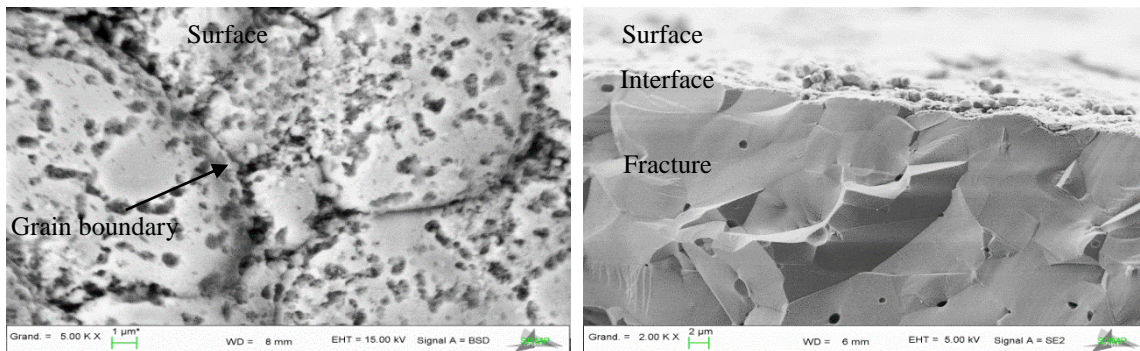


FIGURE 2. SEM observations of surface and fractured cross-section of a poly-crystal after 1000 h at 450 °C and ~ 40 ppm in oxygen.

The porosity level increased gradually with the time during the first few hundred hours of exposure at 550 °C and 1-5 ppm in oxygen. After a few thousands hours, porosity covered the whole surface of the specimen (Figure 1), and the corrosion became almost uniform. Steady corrosion rate was then assumed. The width of the porosity ranged from a few tens to a few hundred nanometers (50-500 nm), offering possibility for the liquid sodium to be trapped. The order of magnitude of the equivalent residual sodium surface layer thickness after ethanol cleaning was in agreement with the observed porosity dimensions as 5 mg/dm² equals ~ 500 nm of pure sodium, so that there was an overall good agreement in between observations and weight variation due to a more efficient sodium residue removal.

Based on the phenomenological observation, the loss of weight was interpreted as an equivalent dissolution reaction that involves the intermediate formation of sodium aluminate (NaAlO₂) with either the solvent or the oxygen impurities (Na or Na₂O). Then, the reaction product dissolved in liquid sodium as a non-negligible solubility of this ternary oxide could reasonably be expected just like other ternary oxide in liquid sodium [15, 16]. Hydrolysis of NaAlO₂ into soluble aluminum hydroxide Al(OH)₃ during the sodium residue removal step was another possibility. Assuming that the overall reaction rate was related to the weight loss of alumina, according to either equation 3 or 4, the quantification of the kinetics based on weight measurement was then possible. Weight losses of sintered alumina were plotted as function of temperature in Figure 3 for 450 °C and 550°C in low oxygen concentration.

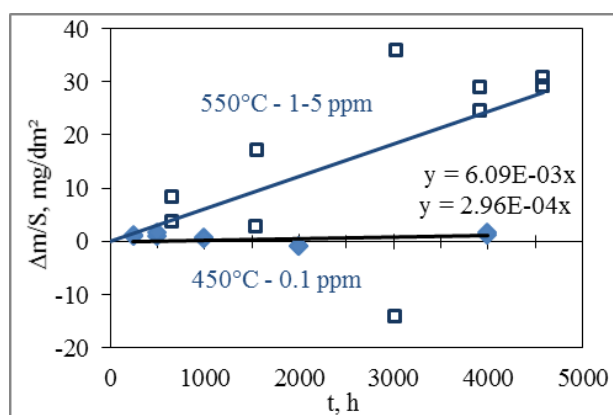


FIGURE 3. Weight loss of sintered alumina at 450°C and 550°C at low oxygen content.

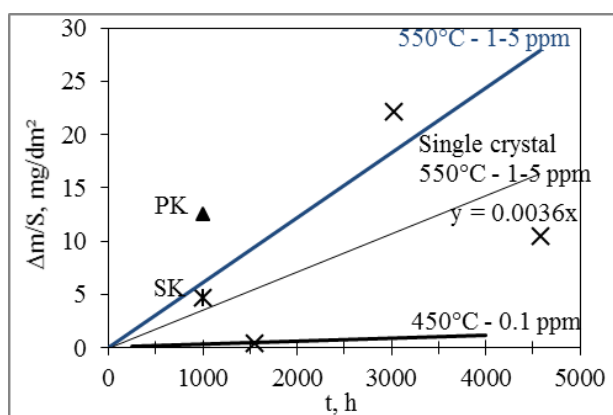


FIGURE 4. Single crystal weight loss at 550°C compared to sintered alumina and literature data (PK, sintered and SK, single crystal at 550°C – 1 ppm [6]).

Because of the difficulty in measuring representative weight loss, the data appeared as scattered and the resulting mean least square regression presented low correlation coefficient for both temperatures. However, it was observed that the weight loss increased with exposure duration. From the assumption that the kinetics was linear, the following weight loss rates could be proposed for low oxygen content:

- 0.14 mg/dm²/d or 1.4 μm/y at 550 °C;
- 0.007 mg/dm²/d or 0.07 μm/y at 450 °C.

The recession depth derived from the weight loss by assuming homogeneous dissolution of the oxide materials and assuming no change in the corrosion mechanism over one year. Despite the scattering of the weight loss data, the homogeneous corrosion kinetics of sintered alumina depended on the temperature as expected. Increasing the temperature from 450 °C to 550 °C increased the dissolution rate by a factor 20. Anyhow, corrosion rates remained small. In fact, the 450 °C rate appeared as almost negligible and close to the uncertainty limit. In addition, the linear fit was somewhat conservative.

Weight losses of single crystals at 550 °C and 1-5 ppm in oxygen are also plotted together with the few available literature data for sintered and single crystal from Kano [6] in Figure 4, measured in a sodium loop:

- Weight loss of a single crystal of high purity is 4.6 mg/dm² for 550 °C -1000 h - 1 ppm in oxygen;
- Weight loss of a sintered alumina of 99.5% purity is 12.6 mg/dm² for 550 °C -1000 h - 1 ppm in oxygen.

If a linear fit was assumed to represent the corrosion kinetics and if the corrosion mechanism remains unchanged over one year, then the corrosion rate was equal to 0.09 mg/dm²/d or 0.8 μm/y at 550 °C for single crystal at low oxygen concentrations. Despite the scattering of the data, this linear regression fit for the single crystal weight loss appeared in good agreement with the literature values. The dispersion could be explained by the surface finishing of

the single crystal since the highest weight loss was measured for the only less polished specimen. The sintered alumina value presented a relative consistency with the linear fit as well, although higher than expected, which might be related to the fact that Na was flowing which could have enhanced the corrosion rate.

From these corrosion rates, the grain boundary effect on the dissolution rates can be assessed by the ratio of the dissolution rates of single crystal and sintered alumina. The dissolution rate appears about twice greater for sintered alumina (10 μm mean size) than for single crystal at 550 $^{\circ}\text{C}$ and low oxygen content (1-5 ppm). The temperature influence was discussed by assessing the corresponding apparent activation energy, to the assumption that the corrosion was correctly represented by the linear corrosion rates noted k: 0.07 $\mu\text{m}/\text{y}$ at 450 $^{\circ}\text{C}$, 1.4 $\mu\text{m}/\text{y}$ at 550 $^{\circ}\text{C}$. Additional value issued from Kano at 650 $^{\circ}\text{C}$ [6] in circulating loop condition and 1 ppm in oxygen for sintered alumina is also taken into account (weight loss 31.3 md/dm² over 1000 h, 0.75 md/dm²/d or 6.9 $\mu\text{m}/\text{y}$ for k). Supposing a linear Arrhenius plot according to the following equation, the linear regression analysis for the slope of $\ln k$ vs. $1/T$ was proportional to the activation energy of the limiting step:

$$k = Ae^{-E_a/RT} \text{ or } \ln k = \ln A - E_a/RT \text{ with } A \text{ the pre-exponential factor and } R \text{ the ideal gas constant (5)}$$

The plot was given in Figure 5 for these only 3 available corrosion rates, and the slope of the linear regression analysis was used to figure out the apparent activation energy, i.e., 130 kJ/mol or 1.35 eV. The order of magnitude of the activation energy is generally supposed to be representative of the limiting step of the corrosion mechanism, which is higher than 50-100 kJ/mol usually observed for chemical reaction control and lower than the 200 kJ/mol expected for solid phase diffusion control [17].

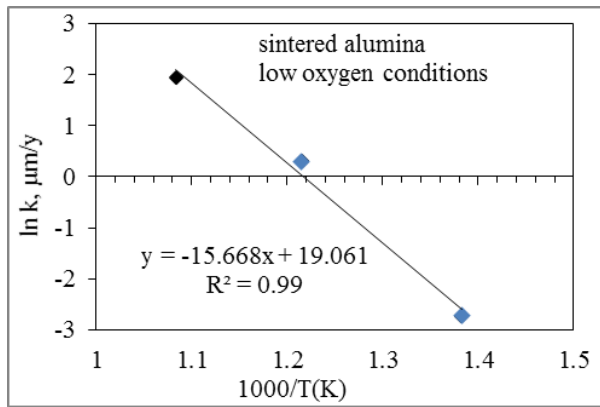


FIGURE 5. Arrhenius plot for alumina poly-crystal at 450, 550 and 650 $^{\circ}\text{C}$ in low oxygen conditions.

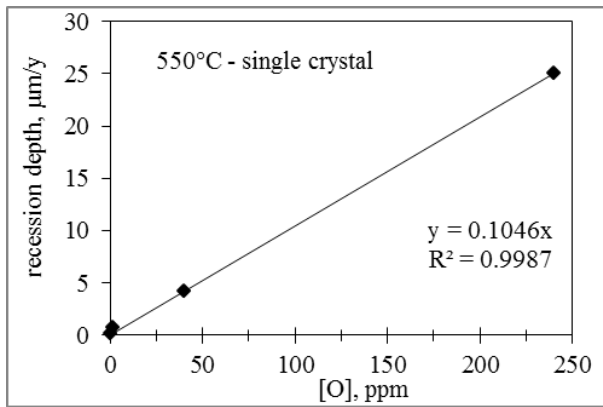


FIGURE 6. Recession depth of single crystal at 550 $^{\circ}\text{C}$ as function of oxygen content in static conditions.

Even if such data should be taken with care, the temperature influence of the ‘dissolution’ rate of sintered alumina by liquid sodium was given for low oxygen conditions, for which no data were yet available to our knowledge in the literature.

Lastly, the effect of dissolved oxygen content was plotted in Figure 6 for the weight loss kinetics at 550 $^{\circ}\text{C}$ of single crystal alumina, assuming linear dissolution rate. The 4 values plotted against the oxygen content were on the same straight line given by linear regression analysis, in agreement with the value given by Kano [6]:

$$R(\text{mg}/\text{dm}^2/\text{d}) = 0.011 \cdot [\text{O}, \text{ppm}] \text{ or } R'(\mu\text{m}/\text{y}) = 0.1046 \cdot [\text{O}, \text{ppm}] \quad (6)$$

This straight dependence with oxygen content allowed concluding that reaction 3 was the main chemical reaction involved in the corrosion mechanism, as well as concluding to a first-order reaction kinetics with respect to oxygen content at the temperature of 550 $^{\circ}\text{C}$.

The intercept point laid within the uncertainty range, so that it was neglected here. However, if reaction 4 occurs, its intensity would be assessed by the intercept point of the linear regression analysis equation, so that it is critical to improve the number of measurement to reduce uncertainty at null value. Indeed, although small, such rates would not be negligible over long-term exposure to liquid sodium.

CONCLUSION

Given these results, and to the restriction of the hypotheses taken, the effects of ‘transients’ oxygen conditions at 550 °C can be assessed to 5 µm loss on sintered alumina for 2000 h exposure at 200 ppm, and to 0.02 µm for 100 h at 15 ppm. For normal operating conditions where the oxygen content is assumed to be buffered to a low but unknown value by the structural steels thanks to the formation of sodium chromite [13,14], the corrosion rate of alumina can be expected to be very low. At 400 °C, the extrapolation gives 0.015 µm/y.

As a conclusion, this study is a first step to a better understanding of the mechanisms of degradation, which is a guide for the fabrication of specific ceramics that would be compatible with the liquid metal.

ACKNOWLEDGMENTS

The CEA R4G project, and in particular F. Serre, C. Cabet and O. Gastaldi are gratefully acknowledged for funding this research, as well as B. Duprey for having provided one weight loss on single crystal obtained on the second testing bench of the Lab (CORRONa-2).

REFERENCES

1. R. Dautray, Y. Bréchet, J. Friedel, *Les fluides caloporteurs pour neutrons rapides*, Les Ulis : Académie des sciences, EDPscience, 2014.
2. Courouau J-L., Balbaud-Céliérier F. , et al., *International Congress on Advances in Nuclear Power Plants*, Nice, France, May 2-5, 2011, ANS.
3. Taylor, R. G.; Thompson, R., *Journal of Nuclear Materials*, 115(1) (1983) 25-38.
4. Fouletier, J., et al. in *Ateliers bilan des actions soutenues GEDEPEON*. 2009. 12-13 Janvier, Paris, France.
5. Macia, F., et al. in *Matériaux 2014*, Nov. 24-28, Montpellier, France.
6. Kano, S., et al., H.U. Borgstedt, Editor. 1995, Plenum Press: New-York. p. 85-94.
7. Mayer, H., *Resistance of oxide ceramic products to corrosive liquids*. 2010 (website <http://friatec.de>)
8. Outoupouku HsC software v5.0
9. Jung, J., A. Reck, and R. Ziegler, *Journal of Nuclear Materials*, 1983. 119(2–3): p. 339-350.
10. Barsoum, M., *Journal of Materials Science*, 1990. **25**(10): p. 4393-4400.
11. Courouau, J-L. et al., in *International Conference on Fast Reactors and Related Fuel Cycles: Safe Technologies and Sustainable Scenarios (FR13)*. 4-7 March, Paris, France.
12. Courouau, J.L., et al. in *ICAPP 2015 (paper 15417)*. 2015. May 03-06, Nice, France.
13. Rouillard, F. et al., in *HTPCM 2016*, 15-20 May, Les Embiez, France.
14. Courouau, J.L., et al. in *EUROCORR 2015 (paper 860)*. 2015. September 6-10, Graz, Austria.
15. Weeks J. R. and Isaacs H. S. in *Chemical aspects of corrosion and mass transfer in liquid sodium*. October 19--20, 1971, Detroit, Michigan, United States.
16. Rivollier, M., et al. .. in *EUROCORR 2015 (paper 733)*. 2015. September 6-10, Graz, Austria.
17. Parry V., In *Technique de l'ingénieur*, M4220, 2015, 10 Décembre.